ACADEMIC PRESS

Journal of Solid State Chemistry 169 (2002) 35–43

JOURNAL OF SOLID STATE CHEMISTRY

www.academicpress.com

Synthesis and characterization of lithium nickel manganese oxides and their delithiated phases

Ramesh Chitrakar,* Shuji Kasaishi, Aya Umeno, Kohji Sakane, Norio Takagi, Yang-Soo Kim, and Kenta Ooi[1]

Institute for Marine Resources and Environment, National Institute of Advanced Industrial Science & Technology, AIST-Shikoku, 2217-14 Hayashi-cho, Takamatsu 761-0395, Japan

Received 5 February 2002; received in revised form 1 July 2002; accepted 20 August 2002

Abstract

Single phases of layered $LiNi_{0.5}Mn_{0.5}O_2$ structure ($a = 2.89$ Å, $c = 14.30$ Å) with the $LiNiO_2$ structure and cubic $Li_{0.4}Ni_{0.3}Mn_{0.3}O$ ($a = 4.15$ Å) with the NiO structure were synthesized by calcination of mixed oxide ($NiMnO_3$) and $LiOH \cdot H_2O$. The optimum calcination temperatures were 1000°C in air for $LiNi_{0.5}Mn_{0.5}O_2$ and 700°C in nitrogen for $Li_{0.4}Ni_{0.3}Mn_{0.3}O$. To our knowledge, the $Li_{0.4}Ni_{0.3}Mn_{0.3}O$ material has not been reported in the literature so far. It was converted to $Li_{0.7}\square_{0.3}Ni_{0.5}Mn_{0.5}O_2$ material ($a = 2.89$ Å, $c = 14.34$ Å) with the $LiNiO_2$ structure by heating at 400°C in air. Acid delithiations of $LiNi_{0.5}Mn_{0.5}O_2$ and $Li_{0.7}\square_{0.3}Ni_{0.5}Mn_{0.5}O_2$ materials were studied using a 0.5 mol dm^{-3} HCl solution at room temperature. The extraction reactions progressed topotactically while maintaining the crystal structures with lithium extraction of 60% in $LiNi_{0.5}Mn_{0.5}O_2$ and 80% in $Li_{0.7}\square_{0.3}Ni_{0.5}Mn_{0.5}O_2$.

Keywords: Lithium nickel manganese oxide; Nickel oxide; Delithiation; Morphology

1. Introduction

In the last 20 years, the synthesis and properties of various lithium manganese oxides with different structures have been reported in the literature. The lithium extraction/insertion reactions of these materials were extensively studied from fundamental standpoints, or for potential use as adsorbents or electrode materials in rechargeable batteries [1–14].

Layered lithium transition metal oxides $LiMO_2$ (M = Mn, Ni, Co) have been the focus of considerable attention for lithium ion battery applications due to their high density and high capacity [8,9,15–17]. Although orthorhombic and monoclinic types of $LiMnO_2$ are promising cathode materials because of their high discharge capacity, these materials are converted to spinel phases during charge and discharge in non-aqueous cells [8,9]. Cationic substitution for nickel appears to be a good method for modifying the structural and electrochemical properties of lithium nickel oxide. In order to improve the specific energy and reduce the material cost of lithium ion cells, many studies have been carried out on the synthesis of new substituted $LiNi_{1-x}M_xO_2$ materials (M = Co [18], Fe [19], Mg [20], etc.) for use as cathode materials to replace the presently used commercial-type $LiCoO_2$.

Li_2MnO_3 has a rock salt structure (monoclinic), which can be related to layer $LiNiO_2$ of space group $R3m$ if the stoichiometry of Li_2MnO_3 is written as $Li(Li_{1/3}Mn_{2/3})O_2$ with one layer of Li and layers of composition $Li_{1/3}Mn_{2/3}$. Manganese and nickel have almost the same ionic radii, and a part of nickel in $LiNiO_2$ can be substituted by manganese to form $LiNi_{1-x}Mn_xO_2$ materials. Although there are several reports related to the incorporation of manganese into $LiNiO_2$ in order to study the electrochemical properties of cathode materials for lithium ion batteries [21–27], there has been no study on the acid delithiation of $LiNi_{0.5}Mn_{0.5}O_2$. $LiNi_{1-x}Mn_xO_2$ materials have been

*Corresponding author. Fax: +81-87-869-3551.

E-mail addresses: chitrakar-ramesh@aist.go.jp (R. Chitrakar), k-ooi@aist.go.jp (K. Ooi).

[1] Also for correspondence.

0022-4596/02/$ - see front matter © 2002 Elsevier Science (USA). All rights reserved.
PII: S0022-4596(02)00014-2

synthesized by different methods such as a solid-state reaction using a mixture of NiO, MnO and $LiOH \cdot H_2O$ [21,22], a solution technique in which a mixed transition metal hydroxide precursor is prepared in oxidative co-precipitation processes prior to the calcination step [24], and a direct co-precipitation method using $Mn(NO_3)_2$, $Ni(NO_3)_2$, LiOH and NH_4OH solutions [23].

In the present study, we report the synthesis of lithium nickel manganese oxides by a two-step method. The first step involves the preparation of mixed oxide ($NiMnO_3$) from a precipitated mixture of Mn-acetate and Ni-acetate heated at 450°C in air. The second step involves the heat treatment of stoichiometric amounts of mixed oxide ($NiMnO_3$) and $LiOH \cdot H_2O$ at high temperature in air ($LiNi_{0.5}Mn_{0.5}O_2$) or nitrogen gas ($Li_{0.4}Ni_{0.3}Mn_{0.3}O$). We found a new phase of composition $Li_{0.4}Ni_{0.3}Mn_{0.3}O$ with the NiO structure, which has not been reported in the literature so far to the best of our knowledge. The conditions for synthesizing these materials, the structural characterization and the acid delithiation were investigated.

2. Experimental

2.1. Preparation of $LiNi_{0.5}Mn_{0.5}O_2$

Stoichiometric mixture of $Mn(CH_3COO)_2 \cdot 4H_2O$ and $Ni(CH_3COO)_2 \cdot 4H_2O$ (1:1 in molar ratio) was dissolved in methanol and the solution was evaporated to dryness. After heating the dried powder at 450°C for 1 h in air, a mixed oxide ($NiMnO_3$) was obtained. Then, stoichiometric amounts of the mixed oxide ($NiMnO_3$) and $LiOH \cdot H_2O$ with Li/(Ni + Mn) equal to 1 in molar ratio were calcined separately at different temperatures for 4 h in air (500°C, 700°C and 1000°C).

2.2. Preparation of $Li_{0.4}Ni_{0.3}Mn_{0.3}O$

A stoichiometric mixture of the mixed oxide ($NiMnO_3$) and $LiOH \cdot H_2O$ with Li/(Ni + Mn) equal to 1 in molar ratio was calcined at 470°C for 2 h in a stream of nitrogen gas and then the temperature was elevated to 700°C and fired for a further 3 h in nitrogen gas. The material was washed with deionized water and dried at 70°C overnight. In order to study the phase transformation of $Li_{0.4}Ni_{0.3}Mn_{0.3}O$, the material was heated at 450°C for 4 h in air.

2.3. Physical analysis

X-ray diffraction (XRD) analysis was carried out using a Rigaku-type RINT 1200 X-ray powder diffractometer using Cu$K\alpha$ radiation with a graphite monochromator and data were collected at room temperature in the range of 2θ between 10° and 70°. The unit-cell parameters were refined by the least-squares method. The errors were ± 0.001 and ± 0.01 Å for a and c lattice parameters, respectively, for the hexagonal structure and ± 0.001 Å for a lattice parameter of cubic structure. DTA-TG curves of materials were measured on a MAC Science Thermal Analyzer (System 001, 200 TG-DTA) at a heating rate of 10°C min^{-1} in air. Water contents of the samples were calculated from the weight loss at 400°C. Infrared spectra were obtained by the KBr pellet method using a Perkin-Elmer System 2000 infrared spectrophotometer. SEM and TEM observations of various materials were carried out on a Hitachi-type S-2460 N scanning electron microscope and JEOL-type JEM-3010 transmission electron microscope, respectively.

2.4. Delithiation of $LiNi_{0.5}Mn_{0.5}O_2$ and heat-treated $Li_{0.4}Ni_{0.3}Mn_{0.3}O$

The delithiation process was carried out by adding 1 g of the solid sample to an aqueous solution of hydrochloric acid (0.5 mol dm^{-3}). The initial molar ratio of H^+/solid sample was 50, indicating that a sufficient quantity of acid was supplied for the delithiation process. The mixture was stirred at room temperature and the sampling (1 cm^3) was done at different intervals of time. After the appropriate dilution, the concentrations of Li, Ni and Mn ions were determined with a Shimadzu AA-760 atomic absorption spectrophotometer. After the extraction reaction, the solid samples were filtered and washed with distilled deionized water and finally dried at 70°C overnight.

2.5. Chemical analysis

Powdered samples (50 mg) were dissolved in 0.5 mol dm^{-3} HCl solution containing 5% H_2O_2 and lithium, nickel and manganese contents were determined. The mean oxidation number of manganese (Z_{Mn}) was evaluated after determining the available oxygen by the standard oxalic acid method [28]. Powdered samples (100 mg) were kept in 10 cm^{-3} of (1 + 4) sulfuric acid and 10 cm^{-3} of standard 0.3 mol dm^{-3} sodium oxalate solution. After dissolving the solid sample at 70°C in water bath, the excess sodium oxalate solution was back titrated with standard 0.1 mol dm^{-3} potassium permanganate solution.

3. Results and discussion

3.1. Characterization of $LiNi_{0.5}Mn_{0.5}O_2$

The XRD patterns of $LiNi_{0.5}Mn_{0.5}O_2$ samples prepared at different temperatures in air are shown in Fig. 1 (left). The peak intensity of the (I_{104}) was higher

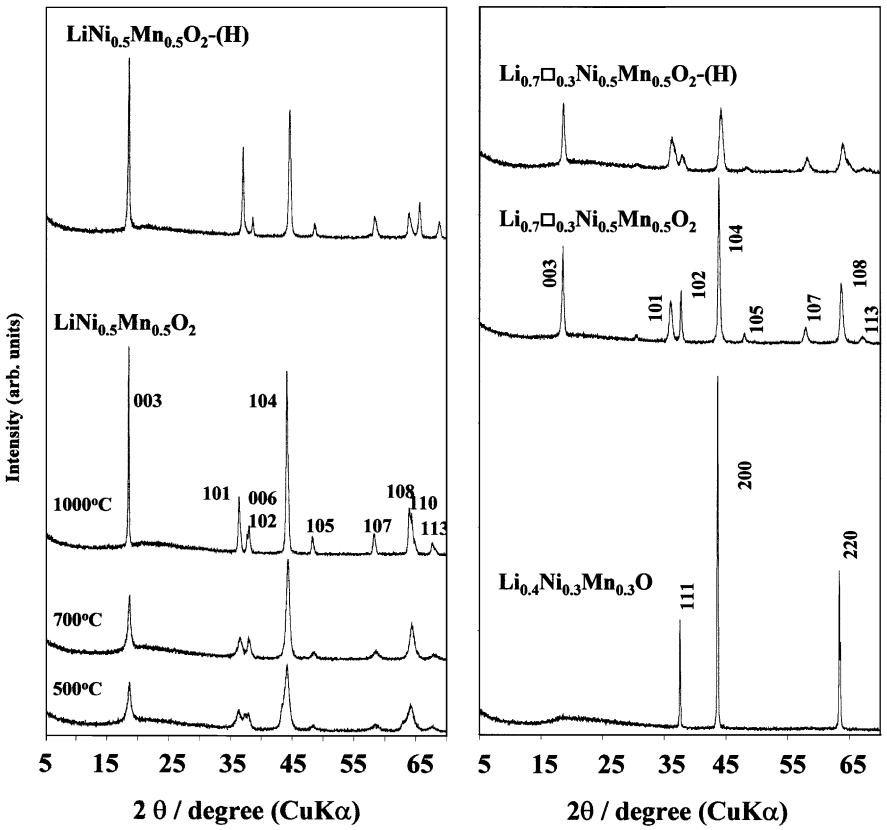

Fig. 1. XRD patterns of $LiNi_{0.5}Mn_{0.5}O_2$ material synthesized at different temperatures in air (left) and $Li_{0.4}Ni_{0.3}Mn_{0.3}O$ material synthesized at 700°C in nitrogen gas and its derivatives (right).

than the (I_{003}) for the samples prepared at 500°C and 700°C. These two XRD patterns were almost similar to $LiNi_{0.5}Mn_{0.5}O_2$ samples prepared at temperature ranges 470–700°C, which were reported by other researcher groups [26]. But the crystallinity was high for the present sample prepared at 1000°C and the peak intensity of the (I_{003}) was higher than the (I_{104}). The XRD pattern of the sample prepared at 1000°C was almost similar to that reported in the literature [27]. We carried out simple simulation of the XRD patterns of $LiNi_{0.5}Mn_{0.5}O_2$ in hexagonal system of space group $R3m$ (S.G.166) with lithium ions at $3a(0,0,0)$ site, nickel and manganese ions at $3b(0,0,0.5)$ site and oxygen at $6c(0,0,0.25)$ site, using program CaRIne Crystallography 3-1. The main peak intensities of the simulated XRD pattern agree with those of the experimentally determined XRD patterns for samples prepared at 500°C and 700°C, but not for sample prepared at 1000°C due to differences in peak intensities of (I_{003}) and (I_{104}). Yoshio et. al [29] have carried out a detailed study on phase diagram based on $LiNiO_2$, $LiMnO_2$ and Li_2MnO_3 system and they have reported that the sample with the composition of $LiNi_{0.5}Mn_{0.5}O_2$ contained trace amounts of Li_2MnO_3 as impurity. Our present sample $LiNi_{0.5}Mn_{0.5}O_2$ may contain Li_2MnO_3 as a minor impurity, because the XRD peaks at 36.36°, 64.30° (2θ) are not clearly separated. The XRD patterns of the present samples showed diffraction peaks similar to that of the layered $LiNiO_2$ with space group $R3m$, which was iso-structural and had the α-$NaFeO_2$ type. The lattice constants of $LiNi_{0.5}Mn_{0.5}O_2$ prepared at 1000°C in air were $a = 2.89$ Å and $c = 14.30$ Å in a hexagonal setting (Table 1).

The ideal structure for the stoichiometric material $LiNi_{0.5}Mn_{0.5}O_2$, which consists of successive layers of lithium, oxygen, nickel and manganese and oxygen ions, is shown in Fig. 2. Li^+ ions are located in the $3a$ sites, Ni and Mn ions in the $3b$ sites and oxygen in the $6c$ sites. Li and Ni, Mn ions occupy the octahedral sites of a cubic close-packed oxygen atom arrangement. In this structure, one (Ni, Mn) plane is sandwiched by two O planes and the stacking of the layers forms the crystal structure. Li ions can occupy all of the available octahedral sites between neighboring O planes. Thus, the crystal is a layered structure due to the periodic stacking of these planes (O–Ni,Mn–O)Li(O–Ni,Mn–O).... This type of crystal structure has been proposed for the $LiNi_{0.5}Mn_{0.5}O_2$ by other groups [21].

The peak intensity ratio (I_{003}/I_{104}) and the lattice parameter ratio (c/a) of the XRD patterns shown in Fig. 1 are plotted against calcination temperature in Fig. 3. Both (I_{003}/I_{104}) and (c/a) ratios were almost unchanged at calcination temperatures of 500°C and

Table 1
Chemical composition of different materials

Material	Mn/Ni	Li/ Mn + Ni	H_2O/Mn + Ni	Z_{Mn}	Formula	Lattice parameters
(1) $LiNi_{0.5}Mn_{0.5}O_2$ Prepared at 1000°C in air	1.00	1.04	—	3.13	$Li_{1.02}Ni_{0.49}Mn_{0.49}O_2$ ($LiNiO_2$ structure)	$a = 2.89$ Å $c = 14.30$ Å
(2) $LiNi_{0.5}Mn_{0.5}O_2$–(H) Delithiated product of (1)	1.15	0.48	0.21	3.96	$\square_{0.10}H_{0.42}Li_{0.48}Ni_{0.46}Mn_{0.53}O_2$ ($LiNiO_2$ structure)	$a = 2.84$ Å $c = 14.44$ Å
(3) $Li_{0.4}Ni_{0.3}Mn_{0.3}O$ Prepared at 700°C in N_2	0.98	0.68	—	3.29	$Li_{0.4}Ni_{0.3}Mn_{0.3}O$ (NiO structure)	$a = 4.148$ Å
(4) $Li_{0.7}\square_{0.3}Ni_{0.5}Mn_{0.5}O_2$ Heat-treated in air of (3)	1.02	0.68	—	3.72	$Li_{0.67}\square_{0.3}Ni_{0.49}Mn_{0.50}O_2$ ($LiNiO_2$ structure)	$a = 2.89$ Å $c = 14.34$ Å
(5) $Li_{0.7}\square_{0.3}Ni_{0.5}Mn_{0.5}O_2$–(H) Delithiated product of (4)	1.14	0.16	0.17	4.16	$\square_{0.46}H_{0.34}Li_{0.17}Ni_{0.49}Mn_{0.56}O_2$ ($LiNiO_2$ structure)	$a = 2.89$ Å $c = 14.27$ Å

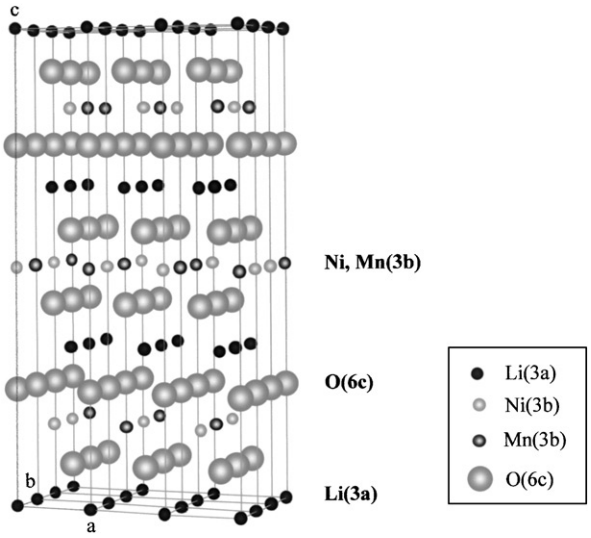

Fig. 2. Ideal structure of $LiNi_{0.5}Mn_{0.5}O_2$.

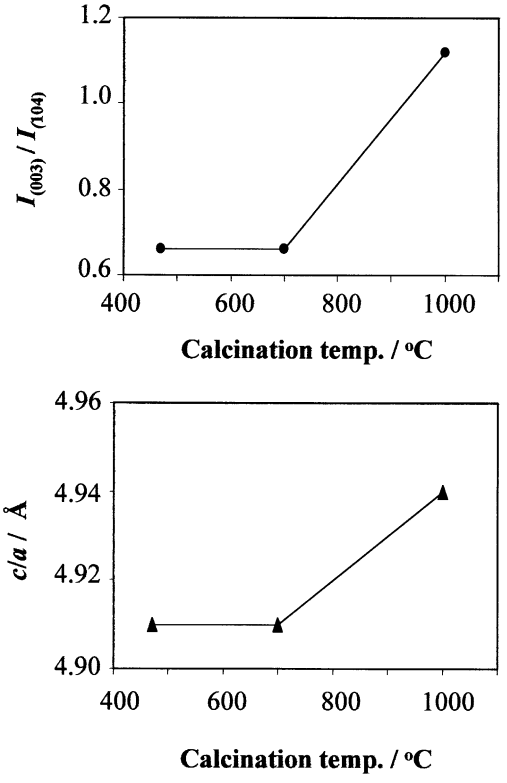

Fig. 3. Variation of intensity ratio of (I_{003}/I_{104}) (top) and lattice parameter (c/a) ratio (bottom) in $LiNi_{0.5}Mn_{0.5}O_2$ as a function of calcination temperature.

700°C, but increased when the temperature was elevated to 1000°C. In general, the substitution of Ni by Mn causes an increase in the degree of cationic disorder in $LiNi_xMn_{1-x}O_2$ materials. Therefore, the cationic disorder between lithium and nickel, manganese ions will increase with a decrease of x from 1 to 0.5. However, Rossen et al. reported that pure single-phase materials could be synthesized for $LiNi_{1-x}Mn_xO_2$ materials with manganese contents $0 \leqslant x \leqslant 0.5$ [21]. It was reported that the peak intensity ratio (I_{003}/I_{104}) depended on the degree of displacement between cations located at 3*a* and 3*b* sites in the space group of *R*3*m* [30]. The larger the ratio (I_{003}/I_{104}), the lesser the cationic disorder. On the basis of these observations, the degree of cationic disorder might be reduced in the present materials when the calcination temperature was elevated to 1000°C in air. Similar trends have been observed in $LiCo_xNi_{1-x}O_2$ materials [30].

Table 1 gives the chemical analysis data of $LiNi_{0.5}Mn_{0.5}O_2$ prepared at 1000°C in air. It shows that the stoichiometry of Li, Ni and Mn corresponded well with that in the relevant target material. The slight lithium excess observed might be due to the coexistence of Li_2MnO_3 as minor impurity.

The SEM images of $LiNi_{0.5}Mn_{0.5}O_2$ revealed plate-like particles with size less than 1 μm, as shown in Fig. 4. In terms of the size of structural regions, TEM detects smaller regions than XRD. Then, we performed direct observations of $LiNi_{0.5}Mn_{0.5}O_2$ by HREM. Fig. 5a (top) is a low-magnification electron micrograph of $LiNi_{0.5}Mn_{0.5}O_2$. Fig. 5a (bottom) is an SAED pattern and an HREM image of the arrow part in Fig. 5a (top). The SAED pattern of the crystal, which is indexed to the

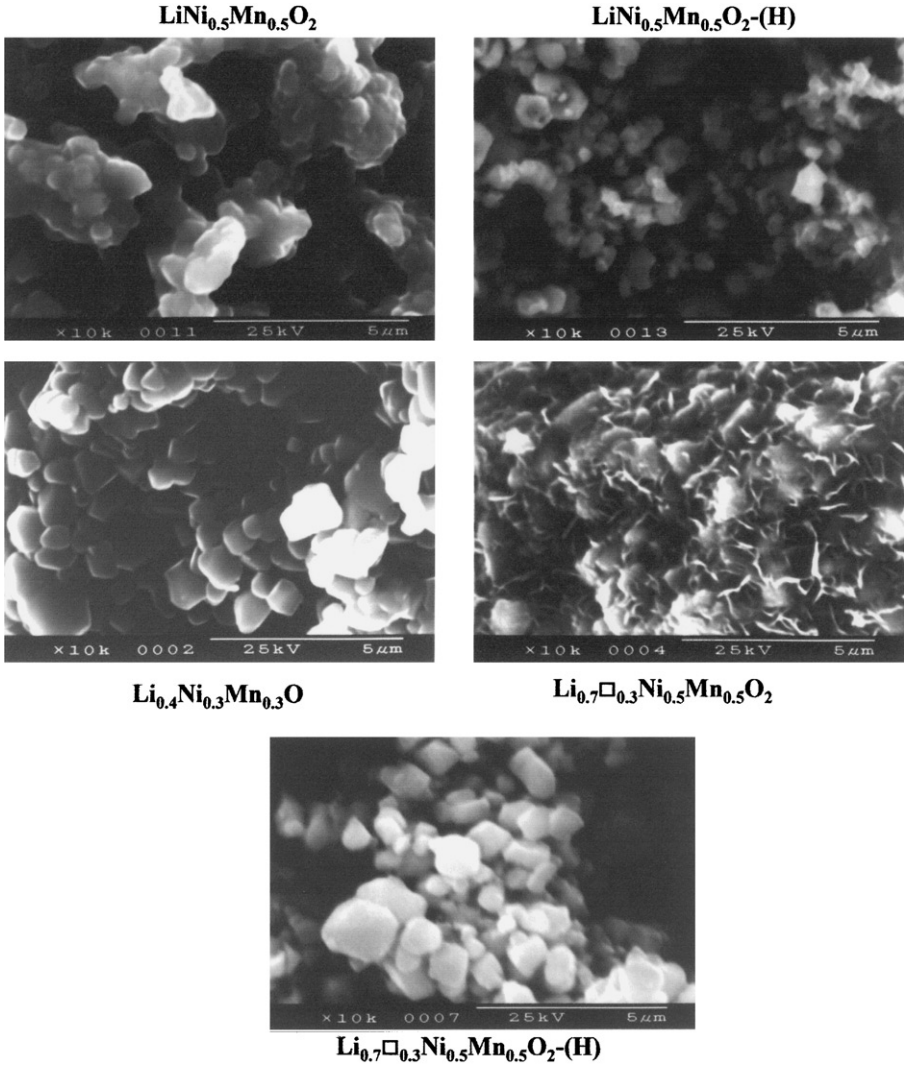

Fig. 4. SEM images of different materials.

[100] direction of the hexagonal structure ($a = 2.89$ Å, $c = 14.30$ Å), is shown in Fig. 5a (bottom). The HREM image of a crystallite in the $LiNi_{0.5}Mn_{0.5}O_2$ sample indicated the presence of a layered structure. The lattice fringes appear along the c-axis in the vertical direction. The layered structure is non-defective, as evidenced by the regular spacing of the lattice fringes in Fig. 5a (bottom). The lattice fringes of the (003) planes ($d = 0.472$ nm) of the layered $LiNi_{0.5}Mn_{0.5}O_2$ structure are indicated in Fig. 5a (bottom). HREM clearly reveals the lattice fringes of the Li layers and the NiMn layers.

The top panel of Fig. 6 shows the FT-IR spectra of $LiNi_{0.5}Mn_{0.5}O_2$ material. Only two absorption bands at 511 and 569 cm^{-1} were observed. Since the vibration of MO_6 octahedra (M = Ni, Mn) generally appears in the frequency range 400–700 cm^{-1}, the absorption bands were assigned to the Ni–O and Mn–O stretching vibrations.

3.2. *Delithiation behavior of* $LiNi_{0.5}Mn_{0.5}O_2$

Fig. 7 (top) shows the delithiation behavior of $LiNi_{0.5}Mn_{0.5}O_2$ in 0.5 mol dm^{-3} HCl solution. Lithium ions could not be extracted completely even after 1 week; the extractability was only 60% with high dissolutions of manganese (12%) and nickel (14%) ions. The delithiation process proceeded by the disproportionation reaction, which can be described similar to that for the $LiNiO_2$ [31]:

$$LiNi_{0.5}Mn_{0.5}O_2 + 4yH^+ \rightarrow (1-y)Li_{(1-2y)/(1-y)}Ni_{0.5}Mn_{0.5}O_2 + 1/2yNi^{2+} + 1/2yMn^{2+} + 2yLi^+ + 2yH_2O.$$

The mole ratio (Li/Ni + Mn) in the supernatant solution after the acid treatment was 1.6, which was slightly low as compared to the theoretical value of 2, based on the

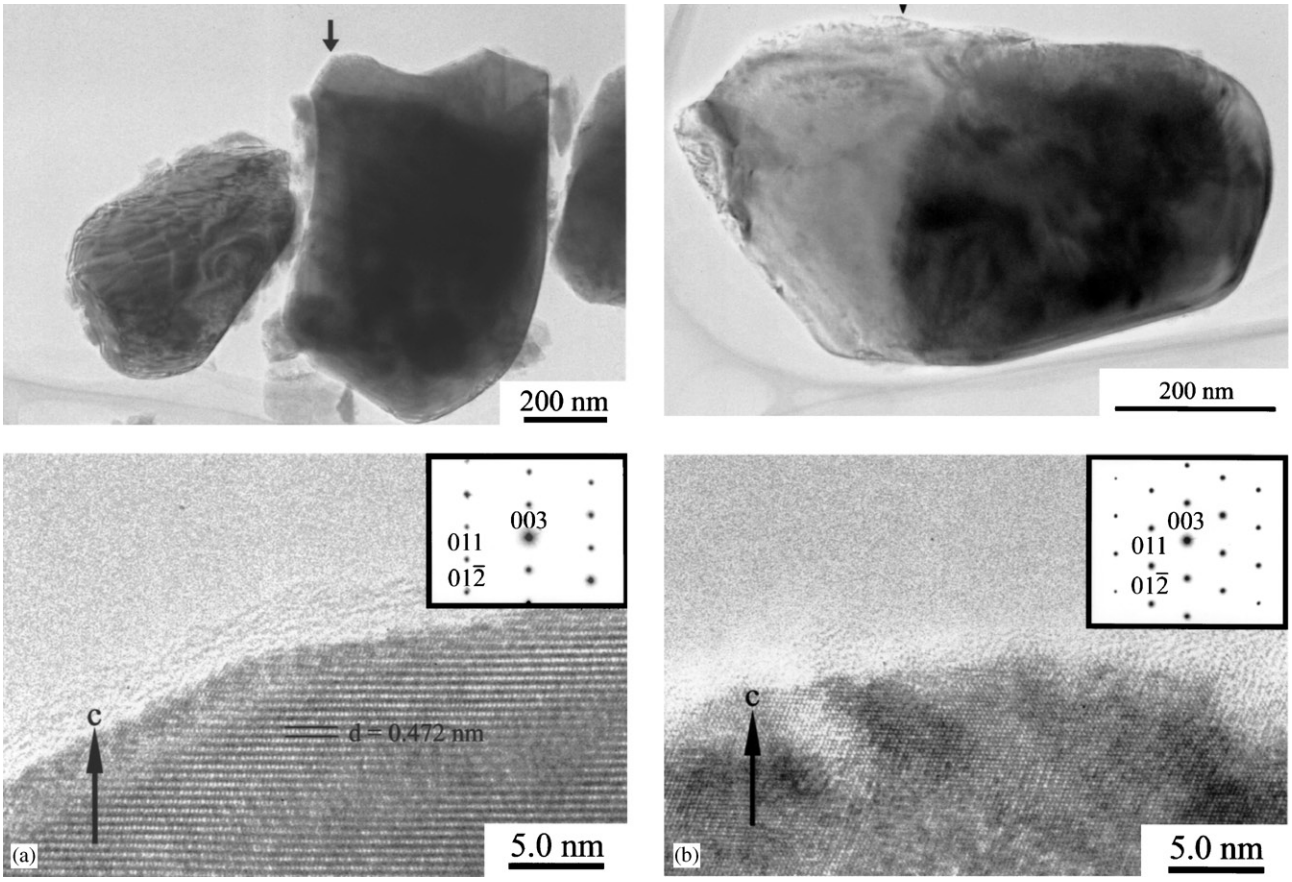

Fig. 5. (a) Low-magnification electron micrograph and HREM with SAED pattern from [100] shown in inset (bottom) of $LiNi_{0.5}Mn_{0.5}O_2$. (b) Low-magnification electron micrograph and HREM with SAED pattern from [100] shown in inset (bottom) of $Li_{0.4}Ni_{0.3}Mn_{0.3}O$.

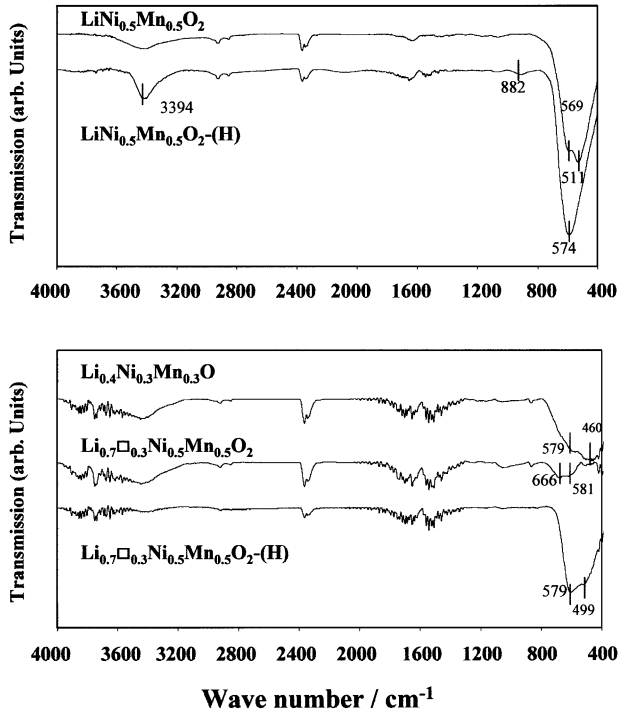

Fig. 6. FT-IR spectra of different materials.

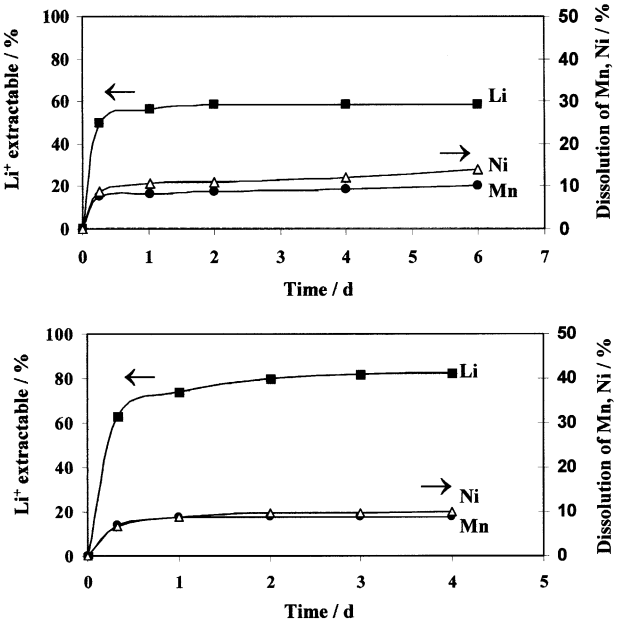

Fig. 7. Extractability of Li^+ ions and dissolution of Mn^{2+} and Ni^{2+} ions from $LiNi_{0.5}Mn_{0.5}O_2$ (top) and $Li_{0.7}\square_{0.3}Ni_{0.5}Mn_{0.5}O_2$ (bottom) with 0.5 mol dm^{-3} HCl solution. Sample = 1.00 g, Vol. of 0.5 mol dm^{-3} HCl = 1 dm^3, Temp. = Room temp.

disproportionation reaction mentioned above. This suggests that the H^+/Li^+ exchange reaction takes place in addition to the disproportionation reaction; the ion-exchange-type extraction reaction has been typically observed for $Li_{1.33}Mn_{1.67}O_4$ [4]. The presence of lattice proton described below supports the occurrence of ion-exchange reaction.

The XRD pattern of partially delithiated material $LiNi_{0.5}Mn_{0.5}O_2$–(H) shows that all of the peaks can be indexed according to the space group *R*3*m*, as shown in Fig. 1 (left top). The lattice parameters ($a = 2.84$ Å and $c = 14.44$ Å) were nearly the same as those of $LiNi_{0.5}Mn_{0.5}O_2$ before acid treatment (Table 1). The SEM image of $LiNi_{0.5}Mn_{0.5}O_2$–(H) shows hexagonal shape with size less than 1 μm (Fig. 4). The lithium extraction proceeded topotactically while maintaining the crystal structure, but changing the particle shape of the original materials. FT-IR spectra of $LiNi_{0.5}Mn_{0.5}O_2$–(H) showed bands at approximately 574, 882 and 3394 cm^{-1} (Fig. 6, top panel). In contrast to that of $LiNi_{0.5}Mn_{0.5}O_2$, only a single band at 574 cm^{-1} was observed in the region between 400 and 800 cm^{-1}, which is attributed to the vibrations of the MO_6 octahedra (M = Mn, Ni). The band around 882 cm^{-1} was due to the lattice coupling vibrations of lattice protons. The absorption band around 3394 cm^{-1} is attributed to the stretching vibration of the hydroxyl group. These results indicate the presence of lattice protons.

Fig. 8 shows the DTA-TG curve of $LiNi_{0.5}Mn_{0.5}O_2$–(H) recorded in air. The initial little weight loss below 200°C is due to the loss of adsorbed moisture. The endothermic peak at 300°C accompanied by the weight loss is due to the loss of lattice protons. This is confirmed by the fact that the as-prepared and the heated samples up to 400°C show the same XRD patterns. A similar endothermic peak has been observed for $H_{1.33}Mn_{1.67}O_4$ obtained by topotactic Li^+ extraction from $Li_{1.33}Mn_{1.67}O_4$ spinel [4]. The weight loss was rarely observed in the temperature range between 400°C and 700°C. The weight loss above 700°C can be ascribed to the loss of oxygen from the lattice accompanied by the reduction of manganese.

The chemical analysis data of the delithiated material obtained by chemically extracting Li from $LiNi_{0.5}Mn_{0.5}O_2$ with 0.5 M HCl solution is shown in Table 1. The data show that complete extraction of lithium was not possible and this can be related to highly crystalline material synthesized at 1000°C. The lattice proton content was evaluated from the weight loss between 200°C and 300°C in the TG curve. The acid treatment resulted in a marked increase in the Z_{Mn} value from 3.16 to 3.96, indicating the oxidation of manganese by the lithium extraction. We have studied the Li^+ extraction reactions with $LiMn_2O_4$, $Li_{1.33}Mn_{1.67}O_4$, $Li_{1.6}Mn_{1.6}O_4$ and $LiMnO_2$ in detail [4,5,32]. In the

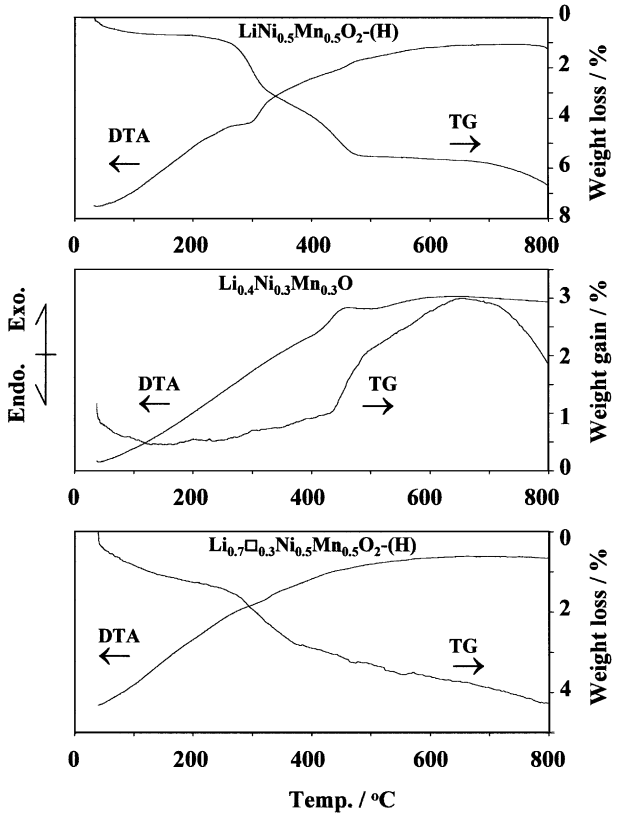

Fig. 8. DTA-TG curves of $LiNi_{0.5}Mn_{0.5}O_2$–(H) (top), $Li_{0.4}Ni_{0.3}Mn_{0.3}O$ (middle) and $Li_{0.7}\square_3Ni_{0.5}Mn_{0.5}O_2$–(H) (bottom).

$LiMn_2O_4$ spinel, a redox-type extraction reaction takes place and tetrahedral vacant sites form after Li^+ extraction, while in $Li_{1.33}Mn_{1.67}O_4$ and $Li_{1.6}Mn_{1.6}O_4$, an ion-exchange-type extraction takes place to form lattice proton. The acid treatment of $LiMnO_2$ results in the redox-type extraction reaction, accompanied by the transformation from orthorhombic to spinel phase. In the present study, the increase of Z_{Mn} indicates the redox-type extraction reaction, while chemical analysis reveals the formation of lattice protons besides the vacant sites. The fraction of vacant sites and lattice proton sites can be roughly estimated from the chemical analysis data as 20% and 80%, respectively. The simultaneous occurrence of lattice proton formation and redox reaction suggests that the disproportionation reaction takes place throughout the particle, preserving the structural framework of $LiNi_{0.5}Mn_{0.5}O_2$, in contrast to the $LiMn_2O_4$ spinel where the disproportionation reaction occurs only at the surface of particles since it belongs to a one-phase solid solution system.

3.3. *Characterization of* $Li_{0.4}Ni_{0.3}Mn_{0.3}O$ *and its heated material*

The reaction in nitrogen atmosphere gives a different structural material. The XRD pattern of the material

synthesized at 700°C in nitrogen gas is shown in Fig. 1 (right). The XRD patterns of cubic and hexagonal structures of NiO are almost similar (JCPDS 4-0835 and 22-1189, respectively). We carried out simple simulation of the XRD patterns for the sample assuming the cubic system with space group *Fm*3*m* (S.G. 225) and the hexagonal system with space group *R*3*m* (S.G. 166) of the NiO structure. The relative peak intensities for the XRD patterns of $Li_{0.4}Ni_{0.3}Mn_{0.3}O$ agree well with those for the simulated XRD patterns of cubic NiO-type structure with Li, Ni, Mn atoms at $4a(0,0,0)$ site and oxygen at $4b(\frac{1}{2},\frac{1}{2},\frac{1}{2})$ site. All of the peaks could be indexed according to the crystal system of cubic structure of NiO with space group *Fm*3*m*. The calculated lattice parameter was found to be $a = 4.15$ Å, which agreed comparatively with that of the cubic type NiO ($a = 4.178$ Å, JCPDS 4-0835). The chemical formula of the material was calculated from the compositional analysis (Table 1). In analogy to the NiO system, the chemical formula of the present materials could be written ideally as $Li_{0.4}Ni_{0.3}Mn_{0.3}O$, where manganese is in the trivalent state, and nickel is in a mixture of divalent (67%) and trivalent (33%) states. We designated the novel material as $Li_{0.4}Ni_{0.3}Mn_{0.3}O$. The SEM images of $Li_{0.4}Ni_{0.3}Mn_{0.3}O$ showed hexagonal-like particles with size less than 1 μm (Fig. 4). TEM images of $Li_{0.4}Ni_{0.3}Mn_{0.3}O$ are shown in Fig. 5b. Fig. 5b (top) is a low-magnification electron micrograph of $Li_{0.4}Ni_{0.3}Mn_{0.3}O$. Fig. 5b (bottom) is an SAED pattern and an HREM image of the arrow part in Fig. 5b (top). It is possible to surmise that $Li_{0.4}Ni_{0.3}Mn_{0.3}O$ is NiO of the cubic structure. Regarding $Li_{0.4}Ni_{0.3}Mn_{0.3}O$, it is understood that the sample is highly crystalline, based on the HREM image.

The DTA-TG curve of $Li_{0.4}Ni_{0.3}Mn_{0.3}O$ is given in Fig. 8 (middle). The weight gain occurring above 200°C till 600°C with a small exothermic peak around 450°C is due to the gain of oxygen by the lattice accompanying the oxidation of Mn from trivalent to tetravalent. The exothermic peak around 450°C corresponds to the structural transformation from NiO-type (cubic) to $LiNiO_2$-type (hexagonal), which can be confirmed from the XRD patterns. The mean oxidation state of manganese increased from 3.29 to 3.72 by the heating at 450°C. The XRD pattern of the material after the heating at 450°C could be identified as a layer structure of *R*3*m* space group with lattice constants of $a = 2.89$ Å and $c = 14.34$ Å. In analogy to the $LiNiO_2$ system, the chemical formula of the heat-treated material could be written ideally as $Li_{0.7}\square_{0.3}Ni_{0.5}Mn_{0.5}O_2$, where manganese has a valence of 3.7, while nickel is in the trivalent state. The deficiency of lithium may be compensated for by the oxidation of manganese to the tetravalent state. The absorption band in the region between 400 and 800 cm^{-1} shows higher values (581 and 666 cm^{-1}) than those for $LiNi_{0.5}Mn_{0.5}O_2$ (Fig. 6). The SEM images showed flower-like particles (Fig. 4).

3.4. Delithiation behavior of $Li_{0.7}\square_{0.3}Ni_{0.5}Mn_{0.5}O_2$

The delithiation behavior of $Li_{0.7}\square_{0.3}Ni_{0.5}Mn_{0.5}O_2$ in 0.5 mol dm^{-3} HCl solution is shown in Fig. 7 (bottom). Lithium extractability was 80% with the dissolution of Mn^{2+} and Ni^{2+} ions after 1 week. A similar disproportionation reaction mentioned above for $LiNi_{0.5}Mn_{0.5}O_2$ may take place because the mole ratio (Li/Ni + Mn) in the supernatant solution after the acid treatment was 1.9, which was comparable to the theoretical value of 2. The XRD patterns of partially delithiated material $Li_{0.7}\square_{0.3}Ni_{0.5}Mn_{0.5}O_2$–(H) show that all of the peaks could be indexed to the *R*3*m* space group with lattice constants $a = 2.89$ Å and $c = 14.27$ Å, the lattice parameters being nearly the same as those of $Li_{0.7}\square_{0.3}Ni_{0.5}Mn_{0.5}O_2$ before the acid treatment (Table 1). The SEM images showed hexagonal-like particles with size less than 1 μm. This suggests that the plates formed on the surface of $Li_{0.7}\square_{0.3}Ni_{0.5}Mn_{0.5}O_2$ were dissolved by the acid treatment. The DTA-TG curve of the acid-treated material is given in Fig. 8 (bottom). The weight loss below 300°C without any peak in the DTA curve is due to the loss of lattice protons. This indicates that a small amount of ion-exchange reaction progresses in this system during the acid treatment, similar to the case of $LiNi_{0.5}Mn_{0.5}O_2$.

4. Conclusion

We propose a new synthetic route for lithium nickel manganese oxides, which comprises a two-step method involving the preparation of a mixed oxide ($NiMnO_3$) followed by calcinations with $LiOH \cdot H_2O$ at high temperatures in air or nitrogen gas. $LiNi_{0.5}Mn_{0.5}O_2$ and $Li_{0.4}Ni_{0.3}Mn_{0.3}O$ materials with structures similar to those of layered $LiNiO_2$ and cubic NiO materials, respectively, could be obtained. Treatment of $LiNi_{0.5}Mn_{0.5}O_2$ and $Li_{0.7}\square_{0.3}Ni_{0.5}Mn_{0.5}O_2$ with 0.5 mol dm^{-3} HCl solution at room temperature for 1 week showed 60% and 80% lithium extractions, respectively, with some dissolution of manganese and nickel ions.

References

[1] J.C. Hunter, J. Solid State Chem. 39 (1981) 142.
[2] X.M. Shen, A. Clearfield, J. Solid State Chem. 64 (1986) 270.
[3] K. Ooi, Y. Miyai, S. Katoh, Solvent Extr. Ion Exch. 5 (1987) 561.
[4] Q. Feng, H. Kanoh, K. Ooi, J. Mat. Chem. 9 (1999) 319.
[5] R. Chitrakar, H. Kanoh, Y. Miyai, K. Ooi, Chem. Mater. 12 (2000) 3151.

[6] R. Chitrakar, H. Kanoh, Y.-S. Kim, Y. Miyai, K. Ooi, J. Solid State Chem. 160 (2001) 69.
[7] R. Chitrakar, H. Kanoh, Y. Miyai, K. Ooi, J. Solid State Chem. 163 (2002) 1.
[8] A.R. Armstrong, P.G. Bruce, Nature 381 (1996) 499.
[9] J.N. Reimers, E.W. Fuller, E. Rossen, J.R. Dahn, J. Electrochem. Soc. 140 (1993) 3396.
[10] Y.-M. Chiang, H. Wang, Y.-I. Jang, Chem. Mater. 13 (2001) 53.
[11] P.S. Whitfield, I.J. Davidson, J. Electrochem. Soc. 147 (2000) 4476.
[12] R.J. Gummow, M.M. Thackeray, J. Electrochem. Soc. 141 (1994) 1178.
[13] B. Ammundsen, D.J. Jones, J. Roziere, Chem. Mater. 10 (1998) 1680.
[14] B. Ammundsen, D.J. Jones, J. Roziere, G.R. Burns, Chem. Mater. 8 (1996) 2799.
[15] A. Rougier, P. Gravereau, C. Delmes, J. Electrochem. Soc. 143 (1996) 1168.
[16] G. Dutta, A. Manthiram, J.B. Goodenough, J.C. Grenier, J. Solid State Chem. 96 (1992) 123.
[17] K. Mizushima, P.C. Jones, P.C. Wiseman, J.B. Goodenough, Mat. Res. Bull. 15 (1980) 783.
[18] C. Delmes, I. Saadoune, Solid State Ionics 53–56 (1992) 370.
[19] J.N. Reimers, E. Rossen, C.D. Jones, J.R. Dahn, Solid State Ionics 61 (1993) 335.
[20] C. Pouillerie, L. Croguennec, Ph. Biensan, P. Willmann, C. Delmes, J. Electrochem. Soc. 147 (2000) 2061.
[21] E. Rossen, C.D.W. Jones, J.R. Dahn, Solid State Ionics 57 (1992) 311.
[22] Y. Nitta, K. Okamura, K. Haraguchi, S. Kobayasi, A. Akira, J. Power Source 54 (1995) 511.
[23] D. Caurant, N. Baffier, V. Bianchi, G. Gregoire, S. Bach, J. Mater. Chem. 6 (1996) 1149.
[24] M.E. Spahr, P. Novak, O. Haas, R. Nesper, J. Power Source 68 (1997) 629.
[25] M. Yoshio, Y. Todorov, K. Yamato, H. Noguchi, J. Itoh, M. Okada, T. Mouri, J. Power Source 74 (1998) 46.
[26] M.E. Spahr, P. Novak, B. Schnyder, O. Haas, R. Nesper, J. Electrochem. Soc. 145 (1998) 1113.
[27] T. Ohzuku, Y. Makimura, Chem. Lett. (2001) 744.
[28] Japan Industrial Standard (JIS), M8233 (1982).
[29] L. Zhang, H. Noguchi, M. Yoshio, J. Power Source 110 (2002) 57.
[30] J. Cho, G. Kim, H.S. Lim, J. Electrochem. Soc. 146 (1998) 3571.
[31] H. Arai, M. Tsuda, K. Saito, M. Hayashi, K. Takei, Y. Sakurai, J. Solid State Chem. 163 (2002) 340.
[32] W. Tang, H. Kanoh, K. Ooi, J. Solid State Chem. 142 (1999) 19.